Massive mobilization of toxic elements from an intact rock glacier in the central Eastern Alps

Hoda Moradi[1], Gerhard Furrer[2], Michael Margreth[3], David Mair[1], and Christoph Wanner[1]

[1]Institute of Geological Sciences, Department of Earth Sciences, University of Bern, Baltzerstrasse 3, 3012 Bern, Switzerland
[2]Institute of Biochemistry and Pollutant Dynamics (IBP), Department of Environmental Systems Science, ETH Zurich, 8092 Zurich, Switzerland
[3]Swiss Federal Institute for Forest, Snow and Landscape Research WSL, Mountain Hydrology and Mass Movements, Zürichstrasse 111, 8903 Birmensdorf, Switzerland

Correspondence: Hoda Moradi (hoda.moradi@unibe.ch)

Abstract. In the central Eastern Alps, an increasing number of high-altitude streams draining ice-rich permafrost display high concentrations of toxic solutes, such as Al, F^-, Mn, and Ni, that may strongly exceed drinking water limits. To obtain novel insights into the causes for the mobilization of toxic solutes and to assess the environmental hazard, here we present a 2-year dataset (2021, 2022) of monitoring a high alpine stream originating from an intact rock glacier located in eastern Switzerland. The monitoring includes monthly sampling and discharge measurements, as well as continuous tracking of the geogenic fluxes of toxic solutes, using a pressure and conductivity probe. Our monitoring revealed high annual fluxes of up to $10\,t\,a^{-1}$ with strong seasonal variations. In particular, the fluxes were highest during the warm summer months and showed strong correlations with hydraulic events such as snowmelt and heavy rainfall. These correlations likely occurred because the mobilization of toxic solutes reflects the last step of a complicated sequence of coupled processes, including (i) the oxidation of sulfides producing sulfuric acid and promoting the dissolution of solutes from the host rock, (ii) temporal storage and long-term enrichment of the dissolved solutes in rock glacier ice, and (iii) their final hydraulic mobilization during climate-change-induced accelerated degradation of rock glaciers. In the studied catchment, the concentrations of toxic solutes strongly exceeded the drinking water limits down to an altitude of 1900 m a.s.l. This depicts a significant hazard for the farmers and their products using the catchment in summer, while the hazard for larger streams in populated areas further downstream is considered limited. Since the fluxes of toxic solutes downstream of rock glaciers likely reflect their final hydraulic mobilization from the solute-enriched rock glacier ice, we hypothesize that flux measurements may serve as a novel environmental tracer to study permafrost degradation.

1 Introduction

Rock glaciers are distinct sediment bodies in high alpine environments often showing a tongue-shaped morphology. They comprise ice and poorly sorted and angular rock debris. Based on their ice content and movement behavior, rock glaciers are categorized into three groups: (i) active rock glaciers, which contain ice and show movement; (ii) inactive rock glaciers, which retain ice but no longer move; and (iii) relict rock glaciers, which neither contain ice nor display movement. Both active and inactive rock glaciers are collectively referred to as intact (Haeberli, 1985; Barsch, 1996; Jones et al., 2019). Active rock glaciers move as a result of the deformation of internal ice, leading to a gravity-driven creep of these landforms (Jones et al., 2019; Giardino and Vitek, 1988; Barsch, 1996). The internal structure of active rock glaciers is composed of three fundamental components. Firstly, there is the active layer, which is a seasonally frozen debris layer, usually several decimeters to a few meters thick (Humlum, 1997). Secondly, beneath the active layer, there is the rock glacier core consisting of a sediment–ice mixture that may contain lenses of pure ice (Ballantyne, 2018).

Thirdly, an unfrozen, fine-grained layer typically occurs at the base of rock glaciers. This base layer acts as aquifer and thus strongly contributes to the high storage capacity of rock glaciers (Hayashi, 2020; Harrington et al., 2018). Therefore, rock glaciers represent valuable long-term freshwater resources and are important for high alpine water budgets (Jones et al., 2018; Wagner et al., 2021b). The current inventory of global rock glacier water volume equivalent has recently been estimated as 83.2 ± 16.64 Gt, representing about 2‰ of the water volume equivalents stored in glaciers when excluding high-latitude cold regions (Jones et al., 2018). Because rock glaciers are more resilient to climatic fluctuations than mountain glaciers, the rapid retreat of the latter will increase the role of rock glaciers as freshwater storage with ongoing climate change (Jones et al., 2019, and references therein; Li et al., 2024). This is supported by the observation that, in arid regions like northern Asia, rock glaciers store up to 4 % of the water equivalent found in mountain glaciers (Jones et al., 2018). A study in Austria suggested an even higher ratio of about 1 : 12 (8.3 %) (Wagner et al., 2021b).

While rock glaciers may become more important for the drinking water supply of high alpine regions (Jones et al., 2019; Wagner et al., 2020, 2021a), the anticipated increase in ice melt export rates may cause serious environmental challenges. In regions with sulfide-bearing (e.g., pyrite) and carbonate-free bedrock, such as in the central Eastern Alps, an increasing number of high-altitude streams originating from intact rock glaciers display high concentrations of toxic solutes, such as aluminum, nickel, manganese, and fluoride, that may strongly exceed drinking water limits (Thies et al., 2007; Ilyashuk et al., 2014; Wanner et al., 2023). Outside the European Alps, the same is observed, for instance, downstream of permafrost areas in the Pyrenees in Spain (Zarroca et al., 2021) or in the Rocky Mountains in the US (Todd et al., 2012). Moreover, elevated solute concentrations have also been observed downstream of ice glaciers (e.g., Fortner et al., 2011; Dold et al., 2013). Most recently, highly acidic conditions and high solute concentrations have additionally been described in seeps draining high-latitude permafrost areas in Alaska, affecting the water quality of streams on the regional scale (O'Donnell et al., 2024). It follows that elevated solute concentrations in water draining from permafrost areas are a global phenomenon (Colombo et al., 2018; Brighenti et al., 2019). High concentrations of toxic solutes impact water quality, thereby affecting humans, plants, and animals (Dos Santos Vergilio et al., 2021; Shaw and Tomljenovic, 2013; Exley, 2016). In particular, they affect fish species and the overall biodiversity in the affected streams (Muniz, 1990; Brighenti et al., 2019; O'Donnell et al., 2024). The adverse water quality of rock glacier springs is often caused by acid rock drainage (ARD), where the weathering of sulfide-bearing minerals, such as pyrite, produces sulfuric acid and therefore promotes the leaching of toxic elements from the crystalline host rocks (Todd et al., 2012; Ilyashuk et al., 2014; Wanner et al., 2018). Microbial activity may

further enhance the rate of sulfide oxidation and hence the production of sulfuric acid (Parbhakar-Fox and Lottermoser, 2017). Recently, however, Wanner et al. (2023) hypothesized that the increased mobilization of toxic solutes from intact rock glaciers observed today additionally requires their temporal storage and long-term enrichment in the rock glacier core (sediment–ice mixture). This is because the oxidation of pyrite and other sulfuric-acid-generating sulfides is kinetically limited (Williamson and Rimstidt, 1994) and because the pyrite content of the studied rock glaciers affected by ARD is rather low (Wanner et al., 2023). This hypothesis is consistent with high concentrations of the same elements (e.g., Ni, Zn, Mn) in the ice of rock glacier cores as those showing high concentrations in rock glacier springs (Nickus et al., 2023). Moreover, it implies that the climate-change-induced accelerated melting of rock glaciers causes a quick and focused export in summer when production rates from ice melt are high and that solute fluxes will increase in the near future.

To verify this storage and enrichment hypothesis and to assess the consequences of accelerated rock glacier degradation on the water quality of high alpine streams, we have initiated a detailed monitoring of a high alpine catchment in the central Eastern Alps in Switzerland. Here, we present monitoring results for the years 2021 and 2022. In contrast to most previous rock glacier monitoring studies focusing on recording solute concentrations (e.g., Williams et al., 2006; Krainer et al., 2007; Brighenti et al., 2021; Wagner et al., 2021a, b; Munroe and Handwerger, 2023), our aim was to systematically record solute fluxes being exported from the intact rock glacier at the origin of the study catchment. The idea behind this approach is that, unlike solute concentrations, fluxes are not affected by an unknown degree of dilution caused by snowmelt and rainwater. Consequently, the collected data provide novel insights into the coupled thermal–hydraulic–chemical processes controlling the discharge and water quality of high alpine streams originating from intact rock glaciers. In the context of global warming, this information is key to assess the environmental hazard caused by ARD in ice-rich permafrost systems such as rock glaciers.

2 Site description

Our flux monitoring is set up along the Aua da Prasüra mountain stream located in the Val Costainas valley in the eastern part of Switzerland, close to the Swiss–Italian border (Fig. 1a). The monitored catchment encompasses a remote area of 9.41 km² at an altitude ranging from 1900 to 2800 m a.s.l. with no mining and almost no other anthropogenic activities apart from alpine livestock farming during summertime. Geologically, the area is part of the crystalline basement of the Austroalpine nappes (Schmid et al., 2004). These basement nappes are pyrite-bearing rocks devoid of carbonate, and they mostly consist of mica-rich, strongly

weathered paragneiss and quartz-rich orthogneiss (Swisstopo, 2024a; Schmid, 1973). Quaternary sediment deposits, consisting of material from these units, such as moraines and alluvial cones, cover a substantial part of the study area. In addition, the catchment is free of ice glaciers, and both intact and relict rock glaciers are frequently present. The Aua da Prasüra stream itself originates from three springs (AP1, AP2, and AP3; Fig. 1), discharging from an ice-rich permafrost zone (Fig. 1b) with the typical morphology of an intact rock glacier (Fig. 2) and occurring at an altitude between 2680 and 2800 m a.s.l. Based on the geological map of the catchment (Fig. 1a) and on a high-resolution digital elevation model resulting from uncrewed aerial vehicle (UAV) imagery (Fig. 2), the surface area of the rock glacier at the origin of the stream is approximately 40 000 m^2 (Fig. 2). A photo of the entire valley is provided in the Supplement (Fig. S2).

As described previously in Wanner et al. (2023), the three rock glacier springs show a typical acid rock drainage (ARD) signature with pH values as low as 5.0 and concentrations of Al, F$^-$, Mn, and Ni exceeding the corresponding drinking water limits by up to 2 orders of magnitude. The discharge from the rock glacier is highest at the spring located at the lowest elevation (AP1, 2660 m a.s.l.). While this spring constantly discharges water, the two others, located at 2700 (AP2) and 2770 (AP3) m a.s.l., respectively, fell dry in late summer during both monitoring years. Downstream of sampling location AP5, the pH and temperature increase to values above 5.5 and 5 °C, respectively, resulting in the precipitation of nanocrystalline basaluminite (Al$_4$OH$_{10}$(SO$_4$) × (H$_2$O)$_5$) because of its strong pH- and temperature-dependent solubility (Wanner et al., 2018, 2023). The precipitation is visible as white coatings on the bedload of the stream (Fig. S1) until the outlet of the catchment, which is about 5 km downstream at an altitude of 1890 m a.s.l. at sampling location AP10 (Fig. 1a). Based on historical aerial photographs, basaluminite precipitation has only occurred since the year 2000 (Wanner et al., 2023). This observation serves as a strong indicator of a significant decline in the water quality of the monitored stream over the past 30 years.

3 Methods

The main aim of our monitoring is to continuously track the fluxes of toxic solutes being transported in the Aua da Prasüra stream. To relate these to the exported fluxes from the intact rock glacier at the origin of the stream, we chose two main monitoring locations: (i) the merging point of the three rock glacier springs at location AP5 and (ii) AP10, located about 5 km downstream of the rock glacier (Fig. 1). With a catchment size of 1.33 km^2, location AP5 corresponds to 14 % of the catchment size monitored at AP10 (catchment area = 9.41 km^2). The AP5 subcatchment includes the entire rock glacier shown in Fig. 2 as well as other ice-rich per-

mafrost areas. To estimate how much of the fluxes measured at AP5 originated from the actual rock glacier, solute fluxes were also periodically measured at AP1_2, located approximately 200 m downstream of AP1. Here the springs from AP1 and AP2 merge and are not affected by AP3 or most of the ice-rich permafrost area outside of the studied rock glacier (Fig. 2).

The monitoring included the collection and analysis of streamwater samples, as well as manual and automated measurements of the stream discharges, as detailed below. Because of the presence of large rock boulders, the seasonally low discharge, and the potential relevance of hidden subsurface flow, reliable discharge and flux measurements at the three rock glacier springs were impossible (AP1, AP2, and AP3; Fig. 1).

3.1 Sampling of streamwater

Streamwater samples were collected from six different locations: AP1, AP2, AP3, AP1_2, AP5, and AP10 (Fig. 1). Sampling took place between May and October of 2021 and 2022, with different sampling intervals. At the most downstream and best accessible location at AP10, samples were collected biweekly and almost throughout the whole year. In the source region, AP1, AP1_2, and AP5, corresponding to the rock glacier spring with the highest discharge and merging points of the rock glacier springs, sampling was carried out approximately every 1.5 months. The two additional rock glacier springs (AP2, AP3) could only be sampled sporadically because they usually fall dry after the termination of the snowmelt in late summer. For all samples, pH, electrical conductivity (EC), and water temperature were measured on site using Hamilton electrodes with Knick Portamess 913 field instruments. The uncertainties of these measurements were 0.1 pH unit and ±5 %. In addition, samples were filtered on site using 0.2 µm filters and were stored in polyethylene bottles. For the analyses of major cations and trace elements, one aliquot per sample was acidified using a 30 % HNO$_3$ solution until the sample had a pH between 2 and 3. All samples were stored at 4 °C prior to analysis.

3.2 Discharge measurements using tracer dilution

At AP1_2, AP5, and AP10, discharge of the stream was measured manually approximately every 1.5 months between May and October of 2021 and 2022. At AP10, discharge measurements were additionally performed in early spring (March–April). These measurements were carried out with the Sommer TQ-S Tracer System using the well-established tracer dilution method with NaCl as the tracer (e.g., Calkins and Dunne, 1970; Day, 1977; Leibundgut et al., 2009) and an uncertainty of ±5 %. Additional details of the tracer discharge measurements are provided in the Supplement (Sect. S1).
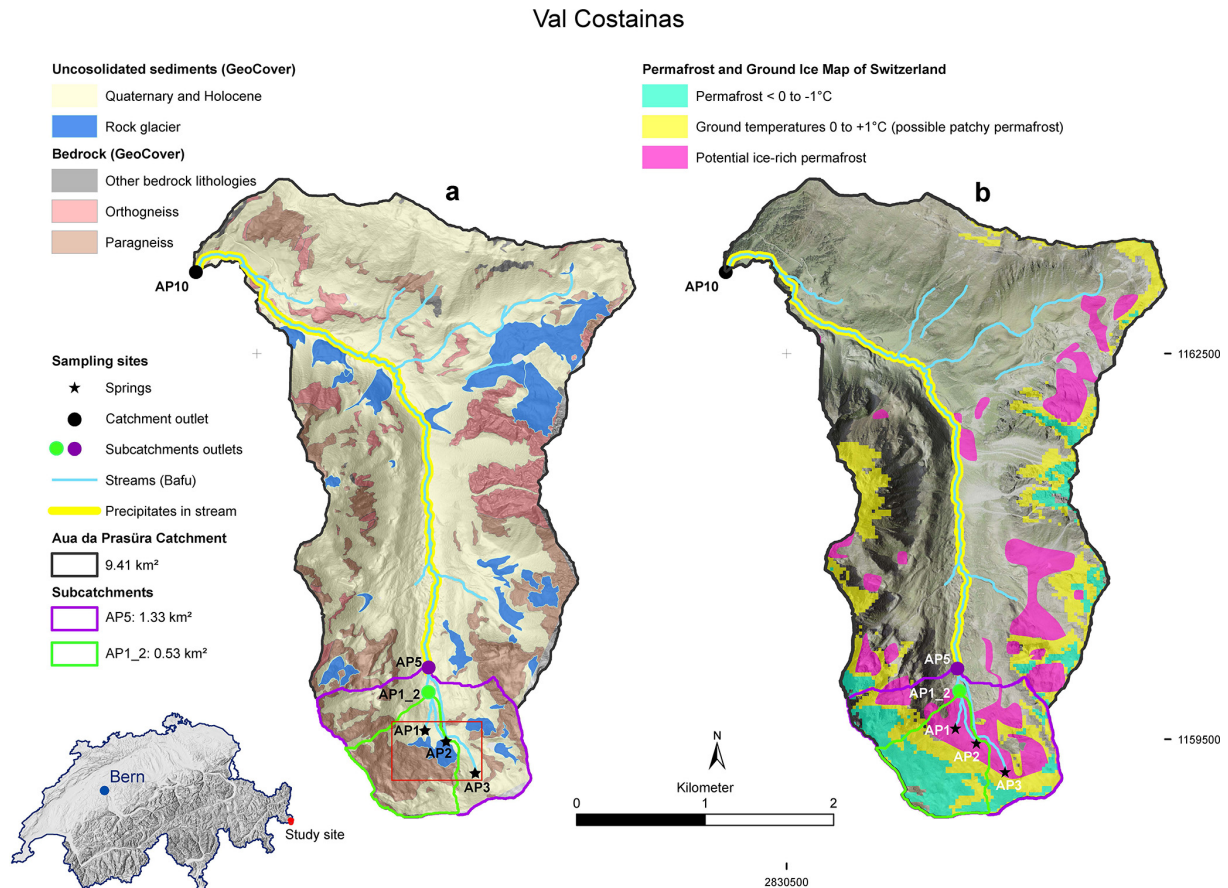
Figure 1. Val Costainas. **(a)** Geological map modified from the GeoCover dataset, map sheet Santa Maria Val Müstair from the Federal Office of Topography (Swisstopo, 2024b) based on field observations, and **(b)** permafrost and ground ice map of the Aua da Prasüra catchment (Kenner et al., 2019). The star symbols refer to the locations of the three rock glacier springs at the origin of the catchment (AP1, AP2, and AP3). The purple- and black-filled circles refer to the two sampling locations downstream of the rock glacier (AP5, AP10), and the green-filled circle is the convergence point of AP1 and AP2, which is called AP1_2. The red rectangle contains the studied rock glacier shown in Fig. 2. The section of the stream with white-coated bedload coatings (i.e., basaluminite; Fig. S1) is highlighted in yellow. Base maps: swissALTI3D digital elevation model and SWISSIMAGE (© swisstopo).

3.3 Automatic water table and electric conductivity measurements

At the AP10 location, the Canton of Graubünden operates a combined water table, temperature, and conductivity probe. The probe takes a measurement of these parameters every 10 min, and the data are published online in real time (ANU, 2024). During wintertime, the discharge of the stream is very low, and the stream is periodically covered by snow and an ice layer, which render the readings of the probe unreliable. With the beginning of the snowmelt season in spring, the discharge increases, and the data recorded by the probe become more reliable. Based on our observations, we considered the recorded data from May to October to be reliable, and we exclusively utilized these measurements for analysis.

3.4 Analytical methods

Water analysis

Concentrations of major cations and anions of the streamwater samples (Na^+, K^+, Ca^{2+}, Mg^{2+}, NH_4^+, F^-, Cl^-, Br^-, NO_3^-, and SO_4^{2-}) were measured by ion chromatography (IC) at the University of Bern using a Metrohm 850 system with a detection limit of $0.1\,\mathrm{mg\,L^{-1}}$ for cations and $0.016\,\mathrm{mg\,L^{-1}}$ for anions. Total inorganic and organic carbon concentrations were determined using a TIC/TOC analyzer (Analytik Jena multi N/C 2100S) with detection limits of $0.1\,\mathrm{mg\,L^{-1}}$ for inorganic carbon and $0.5\,\mathrm{mg\,L^{-1}}$ for organic carbon. Inductively coupled plasma optical emission spectroscopy (ICP-OES) with a Varian 720-ES ICP spectrometer was used to determine aqueous concentrations of Al, Ba, Cu, Fe, Mn, Ni, Zn, Si, Sr, Pb, and Cd. The detection limit was $1\,\mathrm{\mu g\,L^{-1}}$ for Ba, Mn, Sr, and Zn; $3\,\mathrm{\mu g\,L^{-1}}$ for Al and
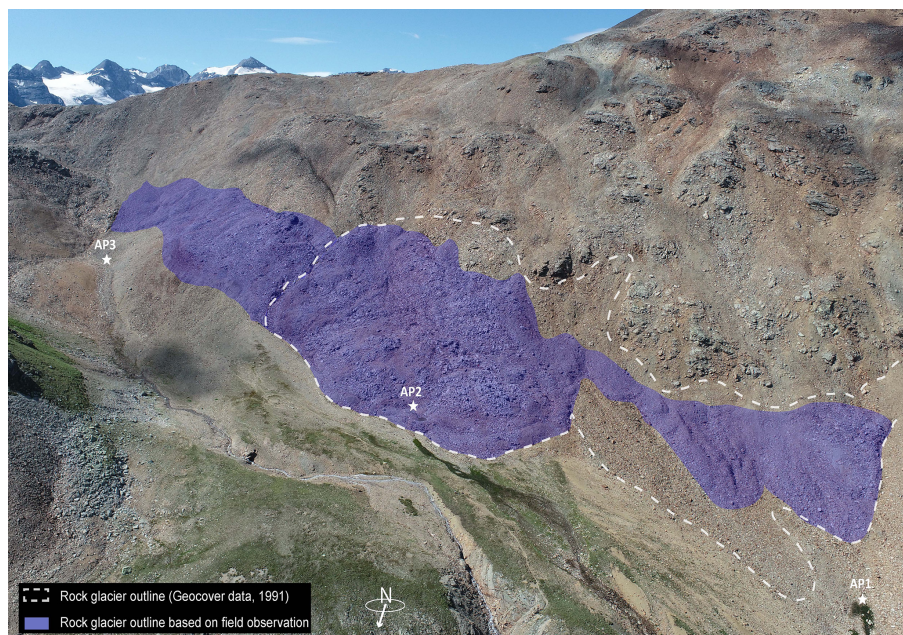
Figure 2. Uncrewed aerial vehicle (UAV) photograph of the entire rock glacier with the three rock glacier springs AP1, AP2, and AP3. The dashed line represents the rock glacier outline based on the GeoCover data shown in Fig. 1a (Swisstopo, 2024b). The blue polygon shows our interpretation of the current rock glacier outline based on field observations. The photograph was captured on 6 July 2022.

Si; $5\,\mu g\,L^{-1}$ for Fe, Ni, Cd, and Cu; and $20\,\mu g\,L^{-1}$ for Pb. Concentrations of As were determined by atomic adsorption spectroscopy (AAS) using a contrAA 700 (Analytik Jena) with a detection limit of $4\,\mu g\,L^{-1}$. The analytical error of all these measurements was within $\pm 5\,\%$.

3.5 Determination of fluxes

At the three discharge monitoring sites (AP1_2, AP5, and AP10), discharge measurements were carried out right after streamwater samples were collected. Accordingly, the fluxes of solutes (e.g., in $mg\,s^{-1}$) corresponded to the product of their concentrations (e.g., in $mg\,L^{-1}$) and the measured discharge (e.g., in $L\,s^{-1}$). Between May and October of 2021 and 2022, our data thus allowed us to determine solute fluxes every 1.5 months. In addition to these sporadic flux determinations, we continuously estimated the fluxes of solutes at the downstream location (AP10) using the continuous water table and electrical conductivity data collected by the installed probe. To do so, water table measurements were correlated with discharge measurements to obtain a discharge–water table relationship (rating curve), allowing us to continuously determine the discharge. Likewise, the electrical conductivity measurements were correlated with solute concentrations measured on the biweekly water samples to establish a conductivity–concentration relationship for the continuous determination of solute concentrations. In the event of the probe malfunctioning, the missing discharge and concentration data at AP10 were reconstructed as detailed in

Sect. S2. The product of discharge and concentration resulted in daily averages of solute fluxes. In this study, we focused on the fluxes of Al, F^-, Zn, Mn, and Ni because these solutes are of the highest environmental concern in streams affected by ARD in the central Eastern Alps (Wanner et al., 2023). Based on the errors of the individual measurements (discharge, electrical conductivity, element concentrations) and the comparison between manual and continuous flux measurements, the uncertainty of the latter was estimated to be within $\pm 10\,\%$.

3.6 Snow height, precipitation, and temperature data

Snow height values for 2021 and 2022 were obtained from the Murtaröl snow station, located approximately 15 km northwest of AP10 at an elevation of 2359 m a.s.l. (SLF, 2024). Similarly, the precipitation and atmospheric temperature data for both years were acquired from the Santa Maria weather station, which is about 6.5 km north of AP10 at an altitude of 1388 m a.s.l. (MeteoSwiss, 2024).

4 Results

4.1 Discharge measurements

The intermittent discharge measurements at the three monitoring locations showed strong seasonal variations (Table 1). The highest values above $50\,L\,s^{-1}$ (AP1_2), $200\,L\,s^{-1}$ (AP5), and $1000\,L\,s^{-1}$ (AP10) were measured during snowmelt in

late spring or early summer (May–July). At AP10, the lowest discharge ($< 70\,\mathrm{L\,s^{-1}}$) was recorded in early spring (March–April), when the winter recession of discharge ended before the snowmelt period started. Owing to the high altitude, no measurement was possible at AP1_2 and AP5 at this time. Accordingly, the lowest discharges at AP1_2 ($< 15\,\mathrm{L\,s^{-1}}$) and AP5 ($< 30\,\mathrm{L\,s^{-1}}$) were measured in early fall in both monitoring years.

In addition to the seasonal discharge variations, the ratio between the discharge at the upstream (AP1_2 and AP5) monitoring sites and the discharge at the downstream (AP10) monitoring site CE2 strongly varied. For AP5, this proportion is provided in Table 1. With the exception of the peak snowmelt period captured on 10 June 2021, the discharge at AP5 relative to that at AP10 was always higher than the 14 % expected from the difference in the corresponding catchment areas. In both monitoring years, the ratio peaked with values above 30 % right after the termination of the snowmelt in early July and hence up to 3 times higher than expected from the two catchment sizes. During low-discharge conditions in fall, the relative discharge at AP5 was still slightly below 20 % and hence at least 1.3 times higher than expected from the area of the two catchments. The continuous discharge data for the downstream location AP10 obtained from the discharge–water table relationship (Sect. S3) are presented with the seasonal flux estimates below.

4.2 Chemical composition of the streamwater

Table 2 presents the concentration range of selected solutes in streamwater samples collected from all six sampling locations. The full analyses are provided in the Supplement (Tables S2–S7). The temperature of the three rock glacier springs at the origin of the Aua da Prasüra stream (AP1, AP2, and AP3; Fig. 1) were constantly below 2 °C, confirming that all springs originate from ice-rich permafrost as indicated by the permafrost and ground ice map shown in Fig. 1b (Kenner et al., 2019). At AP1, AP2, and AP3, the concentrations of Al, F$^-$, Mn, and Ni were almost always above the corresponding drinking water limits. The highest concentrations were found at AP1, discharging at the lowest altitude (2660 m a.s.l.; Figs. 1 and 2). Here, the concentrations reached values up to $28.7\,\mathrm{mg\,L^{-1}}$ Al, $23.1\,\mathrm{mg\,L^{-1}}$ F$^-$, $11.3\,\mathrm{mg\,L^{-1}}$ Mn, and $3.3\,\mathrm{mg\,L^{-1}}$ Ni. In the cases of Mn and Ni, these corresponded to a very strong exceedance of the Swiss drinking water limit by factors of 226 and 165, respectively. For Al and F$^-$, the situation is less severe, but the drinking water limits were still exceeded by factors of up to 143 and 15, respectively. At the other two rock glacier springs (AP2, AP3), the concentrations were lower and decreased with increasing altitude (Table 2). For instance, the maximum concentrations of Ni at AP2 (2700 m a.s.l.) and AP3 (2770 m a.s.l.) were 1.6 and $0.4\,\mathrm{mg\,L^{-1}}$, respectively, and thus 2 and 8 times lower than at AP1. In contrast to the other solutes of interest, the Swiss drinking water limit for

Zn ($5\,\mathrm{mg\,L^{-1}}$) was only periodically exceeded at the lowest rock glacier spring (AP1).

Downstream of the rock glacier springs, the temperature and pH gradually increased, while the solute concentrations decreased as manifested by the streamwater samples collected at AP1_2, AP5, and AP10 (Table 2). Nevertheless, 5 km downstream and at an altitude of 1890 m a.s.l., the concentrations of Mn ($\leq 0.37\,\mathrm{mg\,L^{-1}}$) and Ni ($\leq 0.24\,\mathrm{mg\,L^{-1}}$) at AP10 (Fig. 1) still exceeded the drinking water limits by factors of up to 7 and 12, respectively.

Seasonal variation in concentrations of toxic solutes

At the downstream monitoring location AP10 (Fig. 1), the concentrations of Ni, Zn, and F$^-$ showed strong linear correlations with the electrical conductivity measured by the installed probe as evidenced by linear correlation coefficients (R^2) of at least 0.91 (Fig. 3). The correlations are caused by constant ratios between these concentrations and those of sulfate (Fig. S4). The latter displays by far the highest values of all solutes in our streamwater samples and hence controls the measured EC (Tables 2 and S2–S7). Accordingly, the conductivity data recorded by the probe allowed us to continuously estimate the concentrations of these three solutes using the derived linear calibration curves. For Mn and other reactive solutes, such as Al, the correlation between concentrations and conductivity values was poor (Fig. 3), which means that these concentrations cannot be estimated using the conductivity data.

Figure 4 illustrates the seasonal variations in the EC and the concentrations of F$^-$, Zn, and Ni estimated for the downstream monitoring location AP10 based on the conductivity data and the correlations shown in Fig. 3. The black-filled circles on each curve represent the actual solute concentrations measured on the biweekly collected water samples, demonstrating that the continuously estimated concentrations are reliable. For both monitoring years, these solutes showed maximum concentrations in summer, although the seasonal behavior was slightly different in the 2 years. In 2021, the highest concentrations were estimated for early July followed by a gradual decrease until the end of the monitoring period at the end of October, except for short-term excursions where the concentrations periodically increased. In 2022, with the exception of short negative and positive excursions, the concentrations were nearly constant from early July to mid-September. For both monitoring years, the concentrations at the end of the monitoring period were roughly twice as high as at the beginning of the monitoring period in May. In contrast to the downstream monitoring location AP10, at the upstream monitoring location AP5 and at the most frequently sampled rock glacier spring AP1, the concentrations of the solutes except F$^-$ (i.e., Al, Ni, Zn, and Mn) generally increased during the May–October monitoring period, and the highest values were measured towards the end of the monitoring period (Fig. 5).

Table 1. Discharge measurements at the three monitoring locations and relative discharge contribution of the upstream catchment at AP5 to the discharge of the entire catchment at AP10 (Fig. 1). Also listed is the discharge contribution of AP5 at AP10 (AP5/AP10) and the corresponding normalization using the ratio of the two catchment areas (AP5: 1.33 km^2; AP10: 9.41 km^2).

Date	Discharge at AP1_2 (L s^{-1})	Discharge at AP5 (L s^{-1})	Discharge at AP10 (L s^{-1})	Relative discharge contribution AP5/AP10 (%)	Ratio between relative discharge contribution AP5/AP10 and ratio of the two catchment areas (1.33/9.41)
23 March 2021	–	–	53	–	–
10 June 2021	–	153	1116	14	1
8 July 2021	–	269	629	43	3
18 August 2021	31	58	410	14	1
22 September 2021	14	26	136	19	1.4
21 October 2021	18	34	182	18	1.3
2 April 2022	–	–	64	–	–
20 May 2022	–	–	733	–	–
5 July 2022	52	91	306	30	2.1
13 August 2022	28	47	203	23	1.6
11 October 2022	13	27	140	19	1.4

"–": no measurement possible.
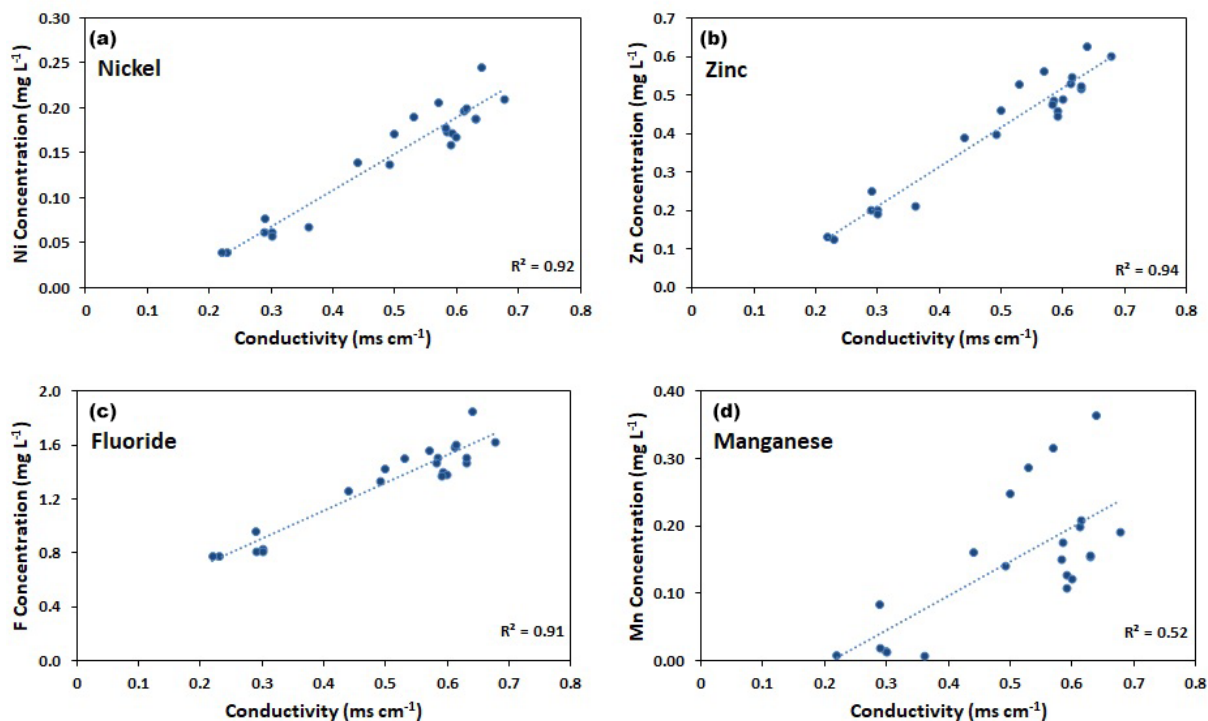
Figure 3. Linear correlations at the downstream monitoring location AP10 between electric conductivity (EC) measured by the installed probe and concentrations of selected solutes. **(a)** Ni. **(b)** Zn. **(c)** F$^-$. **(d)** Mn. Merged data from 2021 and 2022.

4.3 Seasonal evolution of mobilized fluxes

4.3.1 Manual flux measurements (AP1_2, AP5, and AP10)

At the three discharge monitoring locations, AP1_2, AP5, and AP10 (Fig. 1), we took 6, 8, and 10 flux measurements,

respectively. Figure 6 presents the fluxes of Al, F$^-$, Zn, Mn, and Ni. All fluxes showed a very similar pattern with a strong seasonal variation. In both years, the highest fluxes occurred in early July except for AP10, where in 2022 the maximum flux of F$^-$ was observed in May. Among the five solutes, Al and F$^-$ displayed the highest fluxes with values exceeding 100 kg d^{-1} at AP5 in July 2021. On the same sampling day,
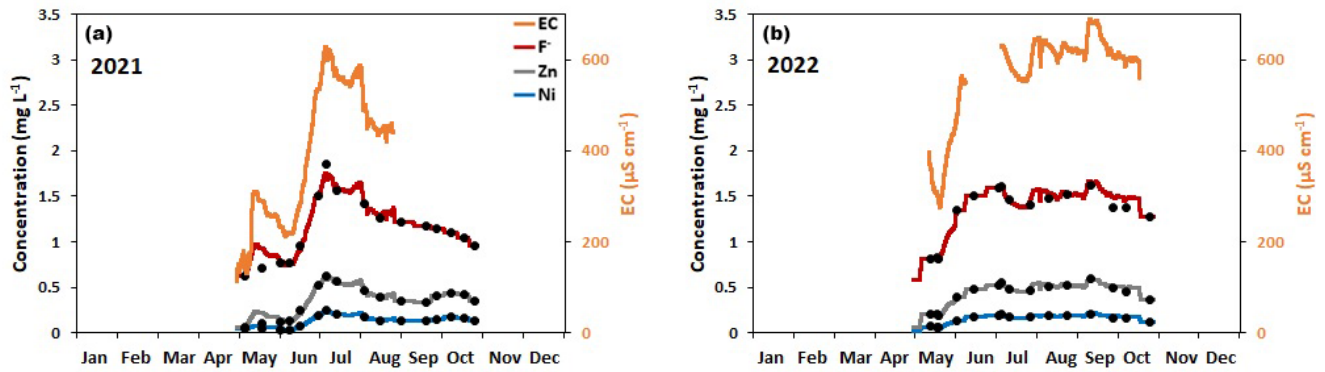
Figure 4. Seasonal evolution of the EC (right-hand *y* axis) and the concentrations of F⁻, Zn, and Ni (left-hand *y* axis) at the downstream monitoring location, AP10, estimated based on the electrical conductivity data and the correlations shown in Fig. 3. **(a)** 2021; **(b)** 2022. The black-filled circles on each curve show the actual solute concentrations measured on the biweekly collected water samples (Table S2). The EC data were not reliable for the following periods: 1 to 14 May 2021, 29 August to 30 October 2021, 1 to 20 May 2022, 7 June to 7 July 2022, and 21 to 30 October 2022. Therefore, a linear interpolation of the chemical analysis of the biweekly samples was employed for these periods to estimate the seasonal evolution of the solute concentrations.
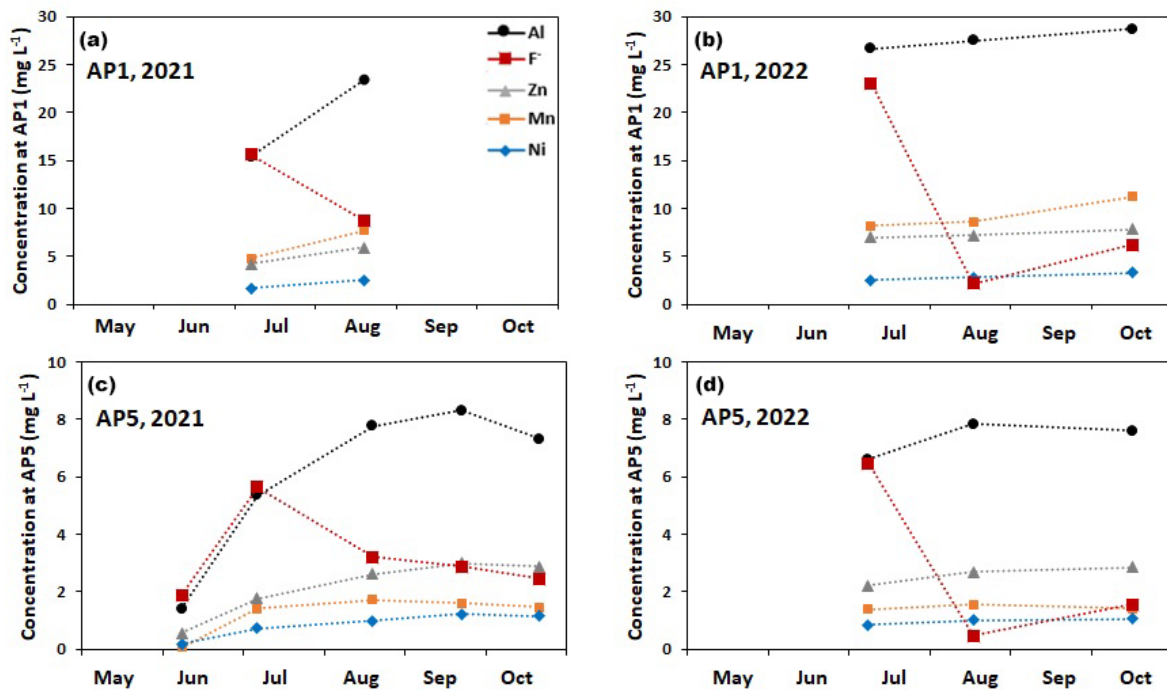
Figure 5. Seasonal variation in the concentrations of Al, F⁻, Zn, Mn, and Ni at the rock glacier spring AP1 and the upstream discharge monitoring location AP5 (Fig. 1). **(a, b)** Interpolation of solute concentrations of samples taken at AP1 in 2021 and 2022, respectively. **(c, d)** Interpolation of solute concentrations of samples taken at AP5 in 2021 and 2022, respectively.

the fluxes of Zn, Mn, and Ni reached maximum values of 20–40 kg d⁻¹. In early and late summer, the fluxes were up to 1 order of magnitude lower.

On specific sampling dates, the three monitoring locations exhibited similar fluxes for Zn and Ni (Fig. 6, Table S1). In contrast, the fluxes of Mn and Al were significantly lower at the downstream location (AP10), while in fall the flux of F⁻ was slightly higher at AP10 than at AP5. These observations

suggest that, at AP10, only the fluxes of Zn and Ni may serve as a proxy for the processes occurring in the rock glacier at the source of the stream (see Discussion below).

4.3.2 Automatic flux estimation (AP10)

The fluxes of Zn and Ni continuously estimated at the downstream monitoring location AP10 are shown in Fig. 7. In-
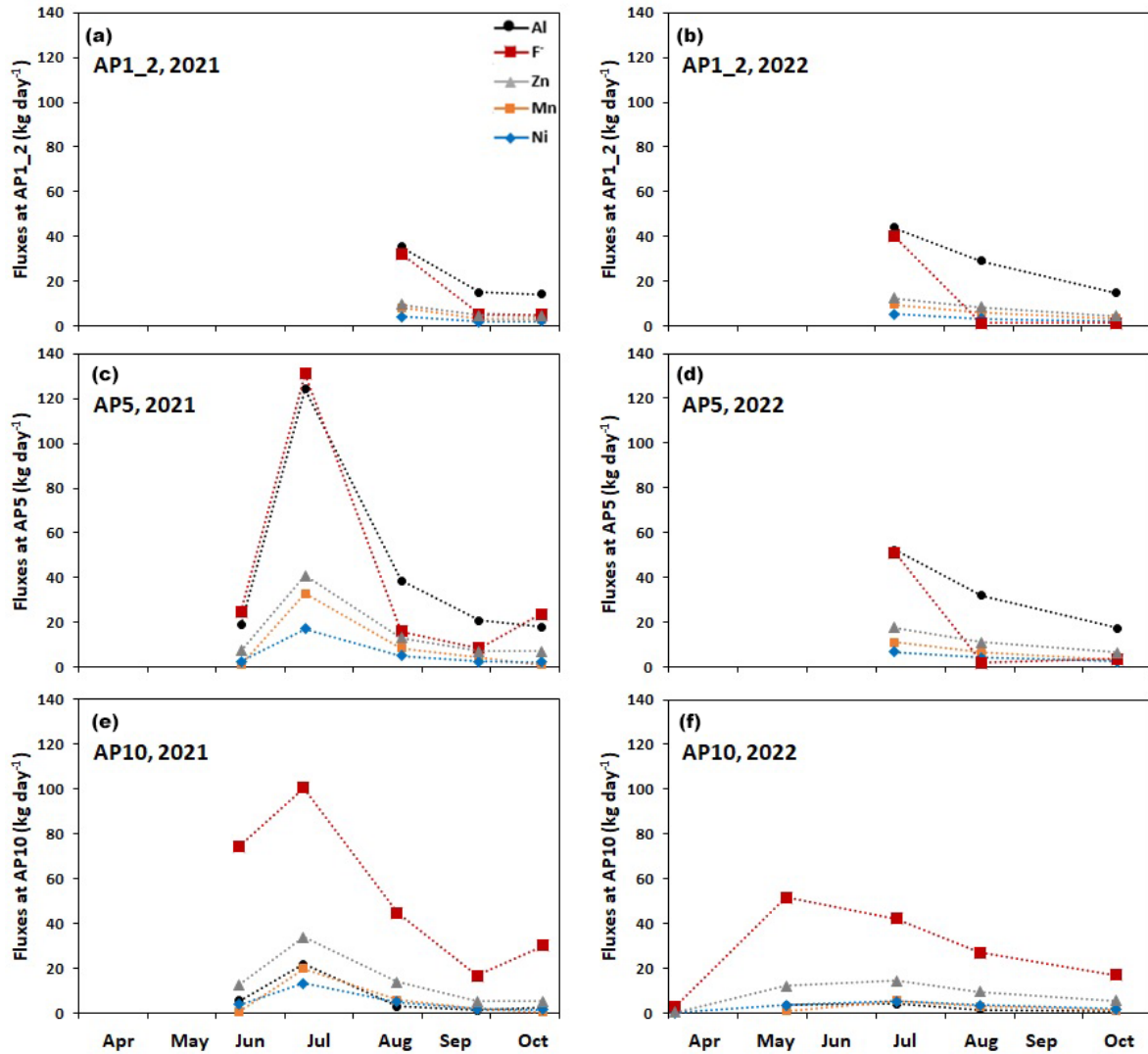
Figure 6. Interpolated fluxes of Al, F⁻, Zn, Mn, and Ni at the three main monitoring stations along the Aua da Prasüra stream. **(a, b)** Fluxes measured at the AP1_2 location in 2021 and 2022. **(c, d)** Fluxes measured at the upstream AP5 location in 2021 and 2022. **(e, f)** Fluxes measured at the downstream AP10 location in 2021 and 2022.

tegrating the fluxes for the 2021 monitoring period yielded surprisingly high total fluxes of 2570 and 940 kg for Zn and Ni, respectively. For the same period in 2022, the total fluxes for these two solutes were 1830 and 650 kg, respectively, and hence 29 %–31 % lower than in 2021.

The seasonality of the estimated Ni and Zn fluxes was rather similar. In both monitoring years, the lowest values were observed at the beginning of the monitoring period in early May when the rock glacier at the origin of the stream was still covered by snow. During snowmelt, the increase in discharge was immediately followed by a rapid surge in the two fluxes, demonstrating a very strong correlation between discharge and solute fluxes. Consequently, synchronous discharge and flux peaks were observed during peak snowmelt conditions (Fig. 7a and b). In 2021, this was the case in mid-June. In 2022, the winter snow cover was less (Fig. 7c), peak snowmelt conditions occurred about 3 weeks earlier at the end of May, and the corresponding discharge and solute fluxes were significantly lower than in 2021. After the snowmelt peaks, additional synchronous flux and discharge peaks occurred during heavy rainfall events. In 2021, this was the case in early July, early August, and early October (Fig. 7d). In 2022, such short-term discharge and flux peaks occurred in response to rainfall events in early July, early August, mid-September, and mid-October. In addition to the simultaneously occurring flux and discharge peaks (Fig. 7a and b), the strong correlation between the two parameters was also manifested by very similar patterns of their seasonal behavior in both monitoring years (Fig. S5).
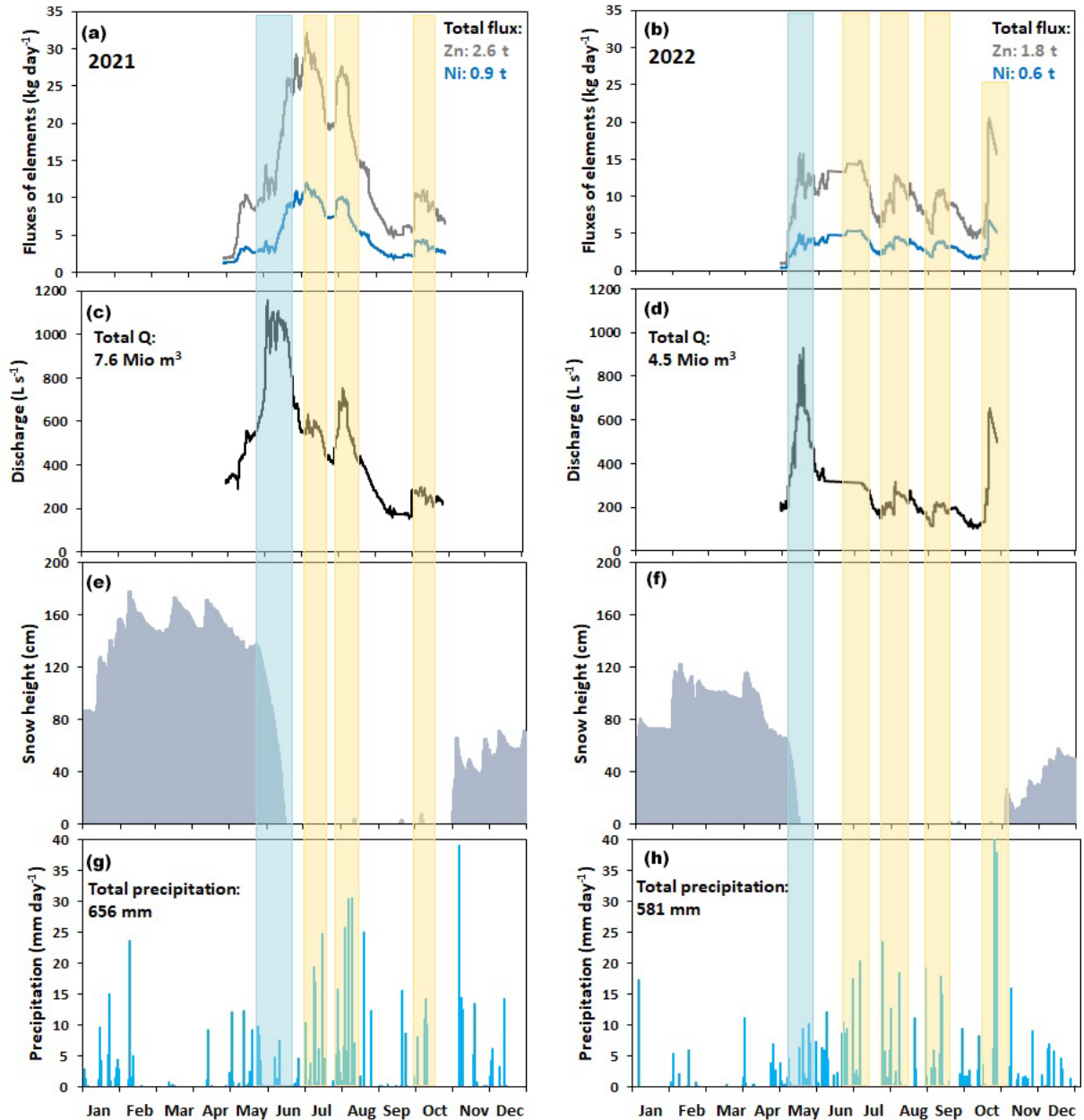
Figure 7. Seasonal evolution of key parameters recorded through the 2 monitoring years. **(a, b)** Fluxes of Zn and Ni calculated for the downstream monitoring location AP10 (Fig. 1) in 2021 and 2022, respectively. **(c, d)** Discharge of the Aua da Prasüra stream measured at the same location (AP10) in 2021 and 2022, respectively. **(e, f)** Snow height recorded in 2021 and 2022 at the Murtaröl snow station (SLF, 2024). **(g, h)** Rainfall recorded in 2021 and 2022 at the Santa Maria weather station (MeteoSwiss, 2024). The light-blue bars highlight synchronous discharge and flux peaks observed during snowmelt peak in June 2021 and May 2022. The yellow bars mark synchronous peaks in discharge and solute fluxes after rainfall events. Due to technical problems, no reliable discharge data were obtained in June 2022. Therefore, a linear interpolation was used to retrieve the data from 7 June to 7 July. Technical problems also occurred from 24 to 31 October 2022 in response to a heavy rainfall event. For this event, a recession curve with $Q_0 = 668\,\mathrm{L\,s^{-1}}$ and $a = 0.00235$ (Eq. S1 in the Supplement) was applied to correct for the missing discharge data.

Table 2. Chemical composition of streamwater samples from different locations along the Aua da Prasüra stream (Fig. 1). Concentrations exceeding the Swiss drinking water limit are written in bold and italics.

Location	Number of samples	Altitude (m a.s.l.)	T (°C)	pH	EC ($\mu s\,cm^{-1}$)	TDS ($mg\,L^{-1}$)	Al ($mg\,L^{-1}$)	Mn ($mg\,L^{-1}$)	Ni ($mg\,L^{-1}$)	Zn ($mg\,L^{-1}$)	As ($\mu g\,L^{-1}$)	F^- ($mg\,L^{-1}$)	$SO_4{}^{2-}$ ($mg\,L^{-1}$)
AP1	5	2660	0.8–1.4	4.7–5.0	1197–2040	1819–3942	*15.4–28.7*	*4.8–11.3*	*1.70–3.30*	*4.20–7.81*	<4–4.1	*2.1–23.1*	1354–2803
AP2	5	2700	0.3–3.1	5.1–5.2	160–711	559–3083	*2.7–10.9*	*0.3–3.4*	*0.35–1.63*	0.74–2.49	< 4	*0.4–5.6*	415–1986
AP3	6	2770	0.7–4.7	5.8–6.4	403–1625	519–1616	*0.5–1.5*	*0.009–0.191*	*0.05–0.39*	0.12–1.16	< 4	*1.4–4.3*	369–1008
AP1_2	6	2545	2.1–7.6	4.8–5.3	1199–1527	1470–2458	*9.4–13.7*	*1.9–3.2*	*1.2–1.8*	2.8–4.2	0.8–11 TSI	*0.5–11.9*	1083–1821
AP5	8	2530	1.4–8.9	5.3–5.7	317–1208	388–1689	*1.4–8.3*	*0.079–1.729*	*0.18–1.22*	0.56–3.01	< 4	*0.5–6.5*	285–1287
AP10	39	1890	0.6–11.4	6.0–8.1	133–440	117–507	*0.01–0.41*	*0.007–0.365*	*0.02–0.24*	0.05–0.62	< 4	*0.5–1.8*	80–327
¹ Drinking water limit							0.2	0.05	0.02	5	0.01	1.5	

¹ https://www.fedlex.admin.ch/eli/cc/2017/153/de (last access: 11 January 2024).

5 Discussion

5.1 Tracking of toxic solute fluxes exported from the studied rock glacier

The observation that the fluxes recorded at AP5 and AP1_2 yielded similar values (Fig. 6, Table S1) implies that the majority of the fluxes measured at AP5 originate from the studied rock glacier (Fig. 2). In case of Ni, 75 %–88 % of the fluxes at AP5 were already recorded at AP1_2, while, for Zn, the contribution from AP1_2 at AP5 ranged between 64 % and 77 % (Table S1). The difference to 100 % is explained by subsurface flow not captured at AP1_2, minor contributions from other ice-rich permafrost features (Fig. 1), and contributions from AP3. The comparison of the Ni and Zn fluxes recorded at AP5 and AP1_2 thus confirms the earlier finding of Wanner et al. (2023) that ice-rich permafrost in general and intact rock glaciers in particular operate as strong and long-lasting chemical reactors causing high concentrations of toxic solutes in the corresponding rock glacier springs.

5.1.1 Conservatively behaving solutes (Ni, Zn)

In the studied system, the strong chemical signal in the rock glacier springs AP1 and AP2 (Table 1) allowed us to continuously track the concentrations and fluxes of conservatively behaving toxic solutes at the well-accessible downstream monitoring location AP10 (Fig. 1). This mainly applied to Ni and Zn as manifested by the observation that, at specific sampling dates, these solutes exhibited similar fluxes at the upstream (AP5) and downstream (AP10) monitoring locations (Fig. 6, Table S1). In general, they were about 5 %–20 % lower at AP10 except for low-flow conditions, when they were up to 35 % lower but did not strongly affect annual fluxes (e.g., September and October 2021 and 2022). Moreover, the quasi-conservative behavior of Zn and Ni along the stream was confirmed by their constant concentration ratios at the two monitoring locations (Fig. S4a and b). This implies that the mobilization of Ni and Zn is not strongly retarded by basaluminite precipitated along the stream, although Ni enrichment in basaluminite has been previously documented (Thies et al., 2017; Wanner et al., 2023). Likewise, this indicates that, downstream of AP5, there are no significant additional sources for these solutes. Thus, the fluxes of Ni and Zn monitored at AP10 exclusively originate from ice-rich permafrost upstream of AP5, whereby the majority (up to 88 %) is exported from the studied rock glacier.

Despite their conservative behavior, the seasonal concentration patterns for Zn and Ni vary along the stream (Figs. 4 and 5). Near the rock glacier source, concentrations of Ni and Zn (and other solutes) display an increasing trend throughout the summer (AP1, AP5; Fig. 6). In contrast, concentration peaks are observed in early summer at the downstream location (AP10; Fig. 5). This contrasting behavior is due to the fact that all concentrations are controlled by the amount of

solutes being mobilized from the rock glacier and the degree of dilution by snowmelt and rainwater. Due to the strong difference in the catchment sizes at these three sampling locations (AP1: 0.04 km^2; AP5: 1.33 km^2; AP10: 9.41 km^2), the degree of dilution is strongly different, causing the observed variation in the concentration patterns along the stream. Because of the strong impact of dilution, we propose that tracking solute fluxes is more useful than solute concentrations to quantitatively understand the seasonality of the mobilization of toxic solutes from the rock glacier. Solute fluxes correspond to the product between solute concentrations and the discharge and hence account for dilution effects by snowmelt and rainwater, which both show strong seasonal variations.

5.1.2 Other solutes (Al, Mn, F$^-$)

In contrast to Ni and Zn, at the downstream monitoring location AP10 (Fig. 1), the fluxes of solutes that do not behave conservatively, or of those affected by additional sources, do not reflect mobilization from ice-rich permafrost upstream of AP5. In the case of Al, this is because most of it precipitates as basaluminite along the stream as manifested by the white bedload downstream of AP5 (Fig. S1). Manganese behaves reactively because the oxidizing conditions in the stream lead to a continuous oxidation and precipitation of Mn, originally mobilized by the reduction of Mn oxides in the rock glacier at the origin of the stream (Wanner et al., 2023). Thus, the concentration of Mn at the downstream location AP10 is not only controlled by the mobilization in the rock glacier but also by the degree of oxidation along the stream, which is a slow, kinetically limited process (Diem and Stumm, 1984). The amount of Mn lost due to oxidation along the stream strongly depends on the seasonally variable residence time of streamwater in the monitored catchment, which is the reason why the correlation between concentration and conductivity is poor (Fig. 3). The flux of F$^-$ (Fig. 7) varies downstream of AP5 because the tributaries merging with the main Aua da Prasüra stream may also contribute to the F$^-$ flux measured at AP10. This is particularly relevant at low-flux conditions in spring and fall, when the fluxes of F$^-$ are usually higher at AP10 than at AP5 (Fig. 6).

Because of their reactive behavior, the total fluxes of Al, F$^-$, and Mn exported from the rock glacier in each monitoring period can only be estimated based on a combination of several data. In particular, these are sporadic manual flux measurements carried out near the rock glacier outlet at AP5; their comparison with the fluxes of Zn and Ni, which are not affected by any chemical reactions occurring along the stream (Fig. 6); and the total fluxes for Zn and Ni estimated at AP10 (Fig. 7a). For Al and F$^-$, this yields annual fluxes about 3 times higher than those estimated for Zn (i.e., up to 10 and 7 t in 2021 and 2022, respectively). For Mn, the annual fluxes exported from the rock glacier were between those of Ni and Zn (2021: 940–2570 kg; 2022: 650–1830 kg).

5.2 Controls on solute mobilization from intact rock glaciers

The very strong correlation between the flux and discharge curves implies that the amount of water infiltrating into the rock glacier system plays a crucial role in controlling the export of solutes from the rock glacier at the origin of the studied stream. This is not only manifested by the simultaneously occurring discharge and flux peaks (Fig. 7a and b) and by the very similar behavior of the flux and discharge curves (Fig. S5), but also by the differences in annual discharge and annual fluxes of toxic solutes calculated for the 2 monitoring years. In 2022, when the total fluxes of Zn and Ni from the rock glacier were about 30 % lower than in 2021, the total discharge between May and October was 41 % lower than in 2021 (Fig. 7c and d). The lower discharge in 2022 resulted from the lower winter snow cover and the lower amount of precipitation in summer (Fig. 7e–h).

Owing to the kinetic limitation of the oxidation rate of pyrite and other sulfuric-acid-generating sulfides (Williamson and Rimstidt, 1994), the very quick increase in solute fluxes observed after hydraulic events (Fig. 7) confirms our hypothesis that processes in addition to chemical weathering (i.e., ARD) are responsible for the high concentrations and fluxes of toxic solutes observed today in the studied catchment (Wanner et al., 2023). Figure 8 presents conceptual models consistent with current thermal, hydraulic, and chemical observations of intact rock glaciers to explain the causes for the highly prominent role of water infiltration on controlling the export of toxic solutes from intact rock glaciers. In particular, the models show that the recorded mobilization of toxic solutes reflects the last step of a complicated sequence of coupled processes, including (i) the oxidation of sulfide, producing sulfuric acid and promoting the dissolution of solutes from the host rock (i.e., ARD), (ii) temporal storage and long-term enrichment of the dissolved solutes in rock glacier ice, and (iii) their final hydraulic mobilization during climate-change-induced accelerated degradation of rock glaciers. The individual steps are described below.

5.2.1 Weathering by sulfuric acid and storage of dissolved solutes in rock glacier ice (Steps (i) and (ii); Fig. 8a)

The current understanding of rock glacier hydrology is that the movement of subsurface water follows two distinct flow paths. In Fig. 8, these are referred to as "quick flow" and "base flow," which occur within the seasonally frozen active layer and the permanently unfrozen base layer, respectively (Giardino et al., 1992; Krainer and Mostler, 2002; Jones et al., 2019). Additionally, subsurface flow through the rock glacier core (i.e., the sediment–ice mixture), known as intra-flow or slow internal flow, was discovered through dye-tracing experiments (Tenthorey, 1992). Furthermore, as reported for the Lazaun rock glacier, temperatures at or even

(a) Past situation: colder climate than today; accumulation of elements
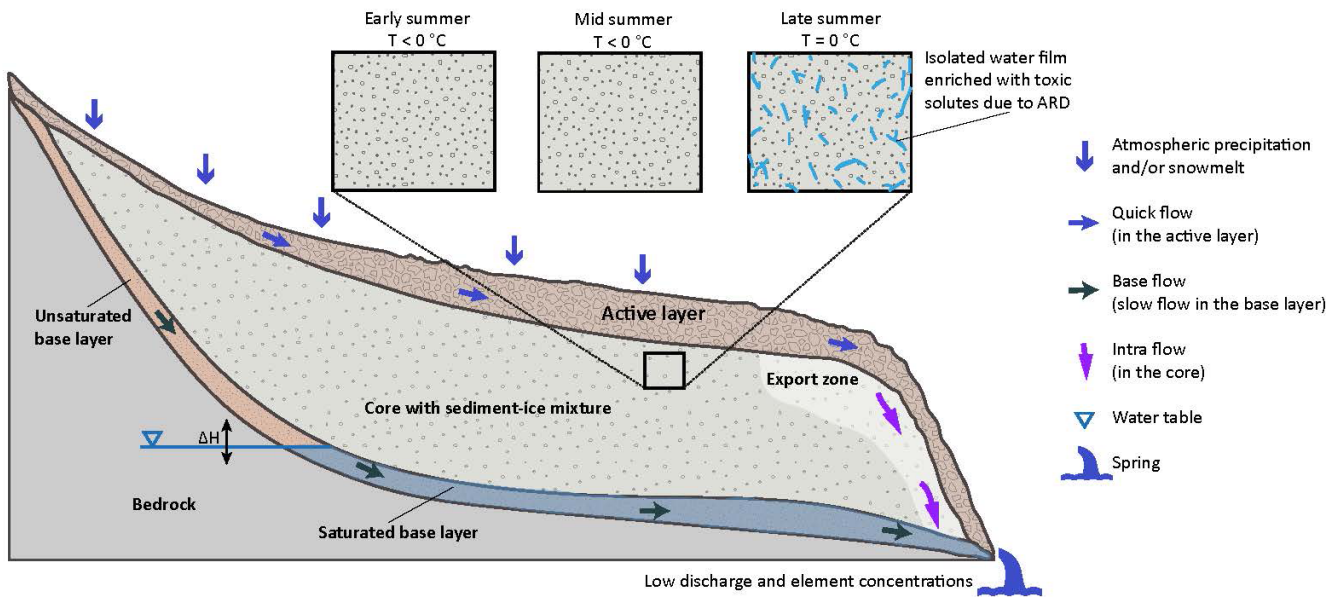
(b) Current situation: degradation of ice and mobilization of elements
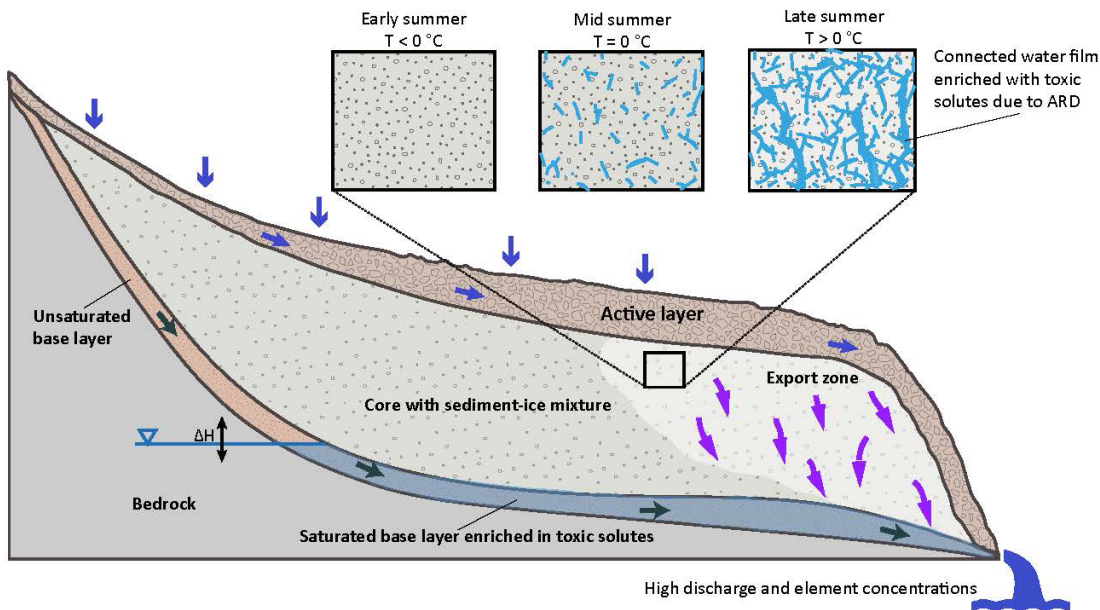
Figure 8. Conceptual schematic models of the coupled thermal–hydraulic–chemical processes controlling the mobilization of toxic solutes from intact rock glaciers affected by ARD. The rectangular boxes illustrate the thermal–hydraulic state at the top of the sediment–ice mixture (i.e., the rock glacier core) in the front part of the rock glacier. **(a)** Situation at high altitude or during climatic conditions where and when the temperature of the cores may reach 0 °C only in late summer. This causes local melting and leads to the formation of isolated and immobile water films, where chemical reactions with the host rock can occur. As a result of multiple seasonal freezing and thawing cycles, toxic solutes become enriched and the amount of ice in the rock glacier remains quasi-constant over time. **(b)** Situation during permafrost degradation, such as today, where the temperature at the top of the rock glacier core already reaches 0 °C in mid-summer (see rectangular boxes). This causes melting and the formation of isolated water films enriched in toxic solutes. In late summer, the temperature becomes positive and the solute-enriched water films become connected. This leads to a gravity-driven vertical export of both ice melt and toxic solutes to the unfrozen and water-saturated base layer (export zone), where the residence time is up to several months. As a consequence, the groundwater in the base-layer aquifer is enriched in toxic solutes. Hydraulic events, such as snowmelt and rainfall, increase the water table (ΔH) in the base-layer aquifer, causing the hydraulic export of water enriched in toxic solutes from the base layer. In late summer, rainfall events additionally accelerate the export of ice melt enriched in toxic solutes from the rock glacier core.

above 0 °C are observed towards the top of the rock glacier core in late summer, i.e., in August and September (Krainer et al., 2015; Nickus et al., 2023), indicating the presence of liquid water promoting intra-permafrost flow. Such fluid flow has mainly been documented in the frontal sections of active rock glaciers, which has significant implications on rates of creep and stability of rock glaciers (Jones et al., 2019, and references therein). In turn, the deformation of rock glacier cores leads to the formation of networks of air voids and fractures, providing positive feedback on intra-permafrost fluid flow (Krainer and Mostler, 2006; Perruchoud and Delaloye, 2007; Ikeda et al., 2008).

The presence of liquid water in rock glaciers is a prerequisite for the chemical interaction with the rock glacier sediments (Wanner et al., 2023). Moreover, it introduces oxygen into the system, promoting the oxidation of sulfides (e.g., pyrite) and thus the generation of sulfuric acid as the main weathering agent. Based on its fine-grained nature and high reactive surface areas, the water-saturated base layer is the obvious candidate for the production of sulfuric acid and strong toxic solute mobilization. Despite a groundwater residence time of several months in the base layer (Jones et al., 2019), however, this is inconsistent with recent experiments showing that the interaction between fine-grained pyrite-bearing paragneiss of the Eastern Alps does not reproduce the high concentrations of toxic solutes in streams discharging from intact rock glaciers (Wanner et al., 2023). Accordingly, toxic solute mobilization must be dominated in other parts of the rock glacier system. Since the active layer mainly consists of large rocks with very low reactive surface areas, the fine-grained sediment–ice mixture in the rock glacier core is the only other plausible alternative.

In the rock glacier core, liquid water (i.e., meltwater) mainly occurs in late summer towards the top and in the front part of rock glaciers because the temperature reaches 0 °C or may even become positive (Krainer et al., 2015; Nickus et al., 2023). If the amount of meltwater is limited and no fully connected water film can develop (Fig. 8a), toxic solutes mobilized from the sediments remain within the rock glacier and their concentrations in rock glacier springs are low. Owing to recurring cycles of freezing and thawing within the sediment–ice mixture, with time this leads to a continuous enrichment and interim storage of the leached solutes in the rock glacier ice. We hypothesize that this scenario is at play at high altitude or under colder climatic conditions than today, where and when the amount of ice in the rock glacier is stable. However, more research is required on how much time for the enrichment of toxic solutes in the rock glacier ice is needed to cause the high solute concentrations currently observed in the studied rock glacier springs. If the climatic conditions are too cold for seasonal temperatures at or above 0 °C, the rock glacier core (sediment–ice mixture) is chemically inert and the accumulation of solutes pauses.

5.2.2 Climate-change-accelerated mobilization of toxic solutes (Step (iii); Fig. 8b)

In recent years, climate warming likely led to an increase in the time when the temperature at the top of the core (sediment–ice mixture) of the studied rock glacier is at or above zero. The same applies to the maximum temperature within the rock glacier in late summer. Consequently, the amount of liquid water (i.e., ice melt) increases, and a fully connected water film enriched in toxic solutes may develop towards the top of the rock glacier core in late summer (Fig. 8b). During this time of the year, this leads to a gravity-driven vertical export of ice melt enriched with toxic solutes to the base layer. During heavy rainfall events, intra-permafrost flow becomes highly significant, and the export to the base layer and also to the rock glacier springs is strongly accelerated. In late summer, this is the main reason for the simultaneously occurring flux and discharge peaks (Fig. 7). Since rock glaciers represent high-altitude aquifers with a high water storage capacity and groundwater residence time on the order of several months (Jones et al., 2019; Wagner et al., 2020, 2021a, b), some of the toxic solutes exported from the rock glacier core are not immediately transported to the rock glacier springs and remain in the unfrozen base layer aquifer during wintertime. As a consequence, the groundwater in the base layer aquifer is enriched in toxic solutes. Stagnant water bodies enriched in toxic solutes may also be present elsewhere in the rock glacier system (i.e., outside the base layer). With the infiltration of snowmelt in the following summer, the water table rises and the hydraulic head gradient in the rock glacier aquifer increases (Fig. 8b). This quickly accelerates the discharge of groundwater and stagnant water enriched in toxic solutes and causes the simultaneously occurring flux and discharge peaks observed during snowmelt (Fig. 7). Such hydraulic mobilization of toxic solutes previously exported from the rock glacier core to the base layer is consistent with the fact that, during snowmelt, the 0 °C isotherm is near the surface (Williams et al., 2006) and that no export of ice melt enriched in toxic solutes to the base layer can happen at this time of the year.

In late summer, when the 0 °C isotherm is below the top of the rock glacier core, the infiltration of rainwater into the system brings thermal energy to the rock glacier core (Rist and Phillips, 2005; Williams et al., 2006), further promoting the degradation of the sediment–ice matrix in addition to the hydraulic effect described above. This is particularly relevant under increased intra-permafrost flow, where the contact area between the ice and water is elevated.

For the studied rock glacier in Val Costainas, the coupled thermal–hydraulic–chemical processes discussed above and shown in Fig. 8 are likely very active. This results in an accelerated degradation of the rock glacier ice accompanied by a strong mobilization of toxic solutes. In particular, this is manifested by the disproportionally high discharge from the rock glacier (Table 1) and the remarkable export rates of

toxic solutes, which are on the order of several tonnes per year (Fig. 7).

5.2.3 Comparison with other conceptual models

It should be noted that other studies have proposed that high concentrations of solutes in rock glacier springs are at least partly due to atmospheric deposition caused by industrial activities or volcanic eruption in addition to ARD (Nickus et al., 2023; Del Siro et al., 2023). Based on the very high solute fluxes currently exported from the studied rock glaciers only covering some $40\,000\,\mathrm{m}^2$ (up to $10\,\mathrm{t\,a}^{-1}$ for trace solutes like Al and F^-; see above), we consider such atmospheric sources not very likely for the studied system. This is consistent with other studies concluding that atmospheric deposition could be excluded as the main cause of high solute concentrations in rock glacier springs (Thies et al., 2007; Steingruber et al., 2021). Moreover, a systematic monitoring of more than 150 rock glacier springs in Austria (Wagner et al., 2019) indicates that the enrichment of elements like Ni, Zn, Mn, and Al and of sulfate occurs primarily in paragneissic geological settings but not in rock glacier of other lithologies, which would likely be the case if atmospheric sources were relevant.

5.3 Environmental implications

The strong mobilization of toxic solutes (Ni, Mn, Al, and F^-) from the studied rock glacier (Fig. 7) represents a hazard to the entire Val Costainas. At the current export rates of up to several tonnes per year, the concentrations of Ni and Mn exceed the corresponding drinking water limits (by 1 order of magnitude) down to an altitude of about 1900 m a.s.l. during the entire summer season, when the catchment is used for alpine livestock farming. As a consequence, the stream cannot be used as a drinking water source. Likewise, the quality of milk products from this farming may be affected because animals frequently drink from the affected stream. Moreover, the elevated concentrations of toxic solutes and low pH values not only degrade the downstream water quality but may also cause significant ecological effects and disruptions in aquatic ecosystems (Thies et al., 2013; Ilyashuk et al., 2018). For instance, Ilyashuk et al. (2018) reported morphological deformities in some aquatic invertebrates due to ARD release into an alpine lake in South Tyrol, Italy. Similarly, the microbial diversity in close vicinity of the stream may be affected (Brighenti et al., 2019; Tolotti et al., 2020, 2024; Sannino et al., 2023). Based on our conceptual model (Fig. 8), the mobilization of toxic solutes will likely increase with accelerated permafrost degradation until reaching a maximum at some point in the future. Owing to the high abundance of pyrite-bearing rocks, the same may apply to areas downstream of intact rock glaciers worldwide. Consequently, the water quality downstream of intact rock glaciers with pyrite-bearing rocks must be carefully monitored. Particularly important is to as-

sess whether the mobilization of toxic solutes affects the water quality of larger streams in populated areas further downstream, acting as regional drinking water resources. At least for the European Alps, however, the risk for such regional contamination is considered limited. This is due to the spatially limited, isolated occurrence of affected rock glaciers at high altitude above 2500 m a.s.l., which is far away from populated areas other than individual farms being operated during the summertime.

In contrast to high-altitude systems, the environmental hazard caused by the degradation of ice-rich permafrost affected by ARD is likely much larger in high-latitude regions, where permafrost occurs at low altitude and hence covers much larger areas. As recently shown for various sites in Alaska, the degradation of permafrost in regions with sulfide-bearing bedrock may decrease the water quality of large streams and thus form a serious threat to the drinking water supply of local communities and aquatic food webs, including subsistence fisheries (O'Donnell et al., 2024). Given that the reported hazard in Alaska only started very recently, it is plausible that the water quality of the studied streams will further decline in the future and form a serious environmental hazard for a large area and a significant number of people. This is particularly the case if the mobilization of toxic solutes from high-latitude permafrost results from the previous accumulation of toxic solutes in the permafrost ice, such as postulated for the rock glacier in Val Costainas.

Although the environmental hazard caused by the mobilization of toxic solutes from rock glaciers in the European Alps may be limited, such mobilization could potentially serve as a novel environmental tracer to study permafrost degradation. This is because, based on our conceptual model (Fig. 8), the fluxes of toxic solutes downstream of rock glaciers essentially reflect their final hydraulic mobilization from the solute-enriched rock glacier ice. Accordingly, all solutes must almost exclusively originate from their interim storage in the rock glacier ice. In contrast, their concentration in snowmelt and rainwater is negligible. It follows that monitoring toxic solute fluxes downstream of rock glaciers may allow us to quantify the export of ice melt from rock glaciers. For instance, the observation that the annual fluxes of Ni and Zn exported from the studied rock glacier were 29 %–31 % lower in 2022 than in 2021 (Fig. 7) suggests that the export of ice melt followed a very similar pattern. This interpretation is remarkable given that 2022 corresponds to a year with record-high temperatures in the Alps (Noetzli and Pellet, 2023), as manifested by much higher summer temperatures than in 2021 (Fig. S5). Moreover, it suggests that, in our study area, the variable infiltration of water into rock glaciers caused by a varying winter snow cover and variations in summer precipitation (Fig. 7) apparently has a much stronger effect on yearly ice melt export rates than the variation in the summer air temperature. To test the significance of toxic solute fluxes as a novel permafrost degradation monitoring proxy or as an essential climate variable (ECV inven-

tory, 2024), more research is required at selected test sites, including long-term solute flux monitoring, the determination of solute concentrations in the rock glacier cores (sediment–ice mixture), and the independent monitoring of rock glacier degradation by other (e.g., geophysical) methods.

6 Conclusions

The detailed, 2-year-long monitoring of a high alpine stream affected by acid rock drainage (ARD) in eastern Switzerland provided novel insights into the causes for the massive mobilization of toxic solutes such as Al, F^-, Zn, Mn, and Ni. The main conclusions and implications are listed below:

– Compared to concentration measurements, the tracking of solute fluxes was more important for increasing our understanding of the mobilization process. This is because, unlike solute fluxes, solute concentrations are influenced by dilution from snowmelt and atmospheric precipitation.

– In the studied catchment, the majority of the toxic solutes are mobilized from an intact rock glacier at the origin of the stream. As a consequence, in the rock glacier springs, their concentrations exceed drinking water limits by factors of up to 226. At 5 km downstream, drinking water limits are still exceeded by factors of up to 15. The corresponding fluxes are on the order of several tonnes per year, which is remarkable given that the surface area of the studied rock glacier only covers an area of around $40\,000\,\text{m}^2$. Furthermore, the high fluxes demonstrate that intact rock glaciers may act as very strong chemical reactors.

– The presence of liquid water in the rock glacier core is required for the production of sulfuric acid as a weathering agent, promoting the dissolution of the toxic solutes from the host rock. Moreover, it introduces oxygen, accelerating pyrite weathering. In the past, recurring cycles of freezing and thawing within the sediment–ice mixture (i.e., the rock glacier core) led to the enrichment and interim storage of the leached solutes in the rock glacier ice. Hence, the presented data fully verified the initial storage and enrichment hypothesis of Wanner et al. (2023).

– Today, climate warming increases the temperature of the top of the rock glacier core, causing the formation of a connected water film enriched in toxic solutes at the interface between sediments and ice in late summer. Infiltration of water from snowmelt and precipitation leads to a quick hydraulic export of both ice melt and toxic solutes. This is manifested by the strong positive correlation between solute fluxes and the discharge.

– In the studied system, the export of ice melt from the rock glaciers currently causes a disproportionally high discharge in summer, confirming that rock glaciers will play a more important role as water resources in alpine regions.

– The fluxes of toxic solutes exported from intact rock glaciers affected by ARD are likely to increase until reaching a maximum. More research is required to estimate when this will be reached and what the maximum concentrations and fluxes will be. This increase in the concentration of toxic solutes corresponds to a decline in water quality downstream of rock glaciers impacted by ARD, emphasizing the necessity for continuous monitoring of such systems. In high-altitude settings such as in the central Eastern Alps, however, the risk for larger streams in populated areas further downstream is considered limited. This is due to the spatially limited, isolated occurrence of affected rock glaciers at high altitude above 2500 m a.s.l., which is far away from populated areas other than individual farms being operated during the summertime. In contrast, the environmental hazard caused by the degradation of ice-rich permafrost affected by ARD is likely much larger in high-latitude regions, where permafrost covers much larger areas.

– As the fluxes of toxic solutes downstream of rock glaciers essentially reflect their final hydraulic mobilization from the rock-solute-enriched rock glacier ice, flux measurements may serve as a novel environmental tracer to study permafrost degradation.

Data availability. Research data can be accessed at https://doi.org/10.5281/zenodo.10558549 (Moradi et al., 2024).

Supplement. The supplement related to this article is available online at: https://doi.org/10.5194/tc-18-1-2024-supplement.

Author contributions. HM and CW designed the study. HM, CW, GF, and MM carried out the sampling and monitoring campaigns. HM performed the chemical analyses of streamwater. HM and CW analyzed the data. HM, with the supervision of CW, wrote the original draft. DM planned the UAV survey and prepared the figures showing maps. CW, GF, DM, and MM reviewed and edited the draft. CW acquired funding and was responsible for project management.

Competing interests. The contact author has declared that none of the authors has any competing interests.

resentation in this paper. While Copernicus Publications makes every effort to include appropriate place names, the final responsibility lies with the authors.

Acknowledgements. We express our gratitude to Priska Bähler, Philipp Hänggi, and Christopher Pichler for their support in the chemical analyses of streamwater. Special appreciation goes to Linda Feichtinger and her team from Biosfera Val Müstair for their dedicated efforts in conducting biweekly water sampling. We also thank Marco Ferrari and David Schmid from the Amt für Natur und Umwelt (ANU), Canton of Graubünden, for maintaining the combined water table and electric conductivity probe used in this study. Review comments by Stefano Brigenthi and an anonymous reviewer greatly helped to improve the clarity of the article.

Financial support. This research has been supported by the Schweizerischer Nationalfonds zur Förderung der Wissenschaftlichen Forschung (grant no. 196847).

Review statement. This paper was edited by Caroline Clason and reviewed by Stefano Brighenti and one anonymous referee.

References

ANU: Hydrodaten, Office for Nature and Environment, Canton of Graübünden, https://www.gr.ch/DE/institutionen/verwaltung/ekud/anu/aktuelles/umweltbeobachtung/hydrodaten/Seiten/Hydrodaten.aspx#/device/UMBRAIL_20/pegel_m, last access: 11 January 2024.

Ballantyne, C. K.: Periglacial Geomorphology, John Wiley & Sons Ltd, ISBN 9781405100069, 2018.

Barsch, D.: Rockglaciers, Springer Berlin Heidelberg, Berlin, Heidelberg, 331 pp., https://doi.org/10.1007/978-3-642-80093-1, 1996.

Brighenti, S., Tolotti, M., Bruno, M. C., Wharton, G., Pusch, M. T., and Bertoldi, W.: Ecosystem shifts in Alpine streams under glacier retreat and rock glacier thaw: A review, Sci. Total Environ., 675, 542–559, https://doi.org/10.1016/j.scitotenv.2019.04.221, 2019.

Brighenti, S., Engel, M., Tolotti, M., Bruno, M. C., Wharton, G., Comiti, F., Tirler, W., Cerasino, L., and Bertoldi, W.: Contrasting physical and chemical conditions of two rock glacier springs, Hydrol. Process., 35, 1–18, https://doi.org/10.1002/hyp.14159, 2021.

Calkins, D. and Dunne, T.: A salt tracing method for measuring channel velocities in small mountain streams, J. Hydrol., 11, 379–392, https://doi.org/10.1016/0022-1694(70)90003-X, 1970.

Colombo, N., Gruber, S., Martin, M., Malandrino, M., Magnani, A., Godone, D., Freppaz, M., Fratianni, S., and Salerno, F.: Rainfall as primary driver of discharge and solute export from rock glaciers: The Col d'Olen Rock Glacier in the NW Italian Alps, Sci. Total Environ., 639, 316–330, https://doi.org/10.1016/j.scitotenv.2018.05.098, 2018.

Day, T. J.: Observed mixing lengths in mountain streams, J. Hydrol., 35, 125–136, https://doi.org/10.1016/0022-1694(77)90081-6, 1977.

Del Siro, C., Scapozza, C., Perga, M. E., and Lambiel, C.: Investigating the origin of solutes in rock glacier springs in the Swiss Alps: A conceptual model, Front. Earth Sci., 11, 1–20, https://doi.org/10.3389/feart.2023.1056305, 2023.

Diem, D. and Stumm, W.: Is dissolved Mn^{2+} being oxidized by O_2 in absence of Mn-bacteria or surface catalysts?, Geochim. Cosmochim. Ac., 48, 1571–1573, https://doi.org/10.1016/0016-7037(84)90413-7, 1984.

Dold, B., Aguilera, A., Cisternas, M. E., Bucchi, F., and Amils, R.: Sources for Iron Cycling in the Southern Ocean, Environ. Sci. Technol., 47, 6129–6136, 2013.

Dos Santos Vergilio, C., Lacerda, D., da Silva Souza, T., de Oliveira, B. C. V., Fioresi, V. S., de Souza, V. V., da Rocha Rodrigues, G., de Araujo Moreira Barbosa, M. K., Sartori, E., Rangel, T. P., de Almeida, D. Q. R., de Almeida, M. G., Thompson, F., and de Rezende, C. E.: Immediate and long-term impacts of one of the worst mining tailing dam failure worldwide (Bento Rodrigues, Minas Gerais, Brazil), Sci. Total Environ., 756, 143697, https://doi.org/10.1016/j.scitotenv.2020.143697, 2021.

ECV inventory: Essential Climate Variable (ECV), Climate Monitoring from Space, https://climatemonitoring.info/ecvinventory/, last access: 8 November 2024.

Exley, C.: The toxicity of aluminium in humans, Morphologie, 100, 51–55, https://doi.org/10.1016/j.morpho.2015.12.003, 2016.

Fortner, S. K., Mark, B. G., McKenzie, J. M., Bury, J., Trierweiler, A., Baraer, M., Burns, P. J., and Munk, L. A.: Elevated stream trace and minor element concentrations in the foreland of receding tropical glaciers, Appl. Geochem., 26, 1792–1801, https://doi.org/10.1016/j.apgeochem.2011.06.003, 2011.

Giardino, J. R. and Vitek, J. D.: The significance of rock glaciers in the glacial-periglacial landscape continuum, J. Quaternary Sci., 3, 97–103, https://doi.org/10.1002/jqs.3390030111, 1988.

Giardino, J. R., Vitek, J. D., and DeMorett, J. L.: A Model of Water Movement in Rock Glaciers and Associated Water Characteristics, in: Periglacial Geomorphology, Binghamton Geomorphology Symposium 22, edited by: Abrahams, A. D. and Dixon, J. C., Taylor & Francis, 26 pp., https://doi.org/10.4324/9781003028901, 1992.

Haeberli, W.: Creep of mountain permafrost: internal structure and flow of alpine rock glaciers, Mitteilungen der Versuchsanstalt fur Wasserbau, Hydrol. und Glaziologie an der Eidgenoss. Tech. Hochschule Zurich, 1985.

Harrington, J. S., Mozil, A., Hayashi, M., and Bentley, L. R.: Groundwater flow and storage processes in an inactive rock glacier, Hydrol. Process., 32, 3070–3088, https://doi.org/10.1002/hyp.13248, 2018.

Hayashi, M.: Alpine Hydrogeology: The Critical Role of Groundwater in Sourcing the Headwaters of the World, Groundwater, 58, 498–510, https://doi.org/10.1111/gwat.12965, 2020.

Humlum, O.: Active layer thermal regime at three rock glaciers in Greenland, Permafrost Periglac., 8, 383–408, https://doi.org/10.1002/(SICI)1099-1530(199710/12)8:4<383::AID-PPP265>3.0.CO;2-V, 1997.

Ikeda, A., Matsuoka, N., and Kääb, A.: Fast deformation of perennially frozen debris in a warm rock glacier in the Swiss Alps:

An effect of liquid water, J. Geophys. Res.-Earth, 113, 1–12, https://doi.org/10.1029/2007JF000859, 2008.

Ilyashuk, B. P., Ilyashuk, E. A., Psenner, R., Tessadri, R., and Koinig, K. A.: Rock glacier outflows may adversely affect lakes: Lessons from the past and present of two neighboring water bodies in a crystalline-rock watershed, Environ. Sci. Technol., 48, 6192–6200, https://doi.org/10.1021/es500180c, 2014.

Ilyashuk, B. P., Ilyashuk, E. A., Psenner, R., Tessadri, R., and Koinig, K. A.: Rock glaciers in crystalline catchments: Hidden permafrost-related threats to alpine headwater lakes, Global Change Biol., 24, 1548–1562, https://doi.org/10.1111/gcb.13985, 2018.

Jones, D. B., Harrison, S., Anderson, K., and Betts, R. A.: Mountain rock glaciers contain globally significant water stores, Sci. Rep.-UK, 8, 1–10, https://doi.org/10.1038/s41598-018-21244-w, 2018.

Jones, D. B., Harrison, S., Anderson, K., and Whalley, W. B.: Rock glaciers and mountain hydrology: A review, Earth-Sci. Rev., 193, 66–90, https://doi.org/10.1016/j.earscirev.2019.04.001, 2019.

Kenner, R., Noetzli, J., Hoelzle, M., Raetzo, H., and Phillips, M.: Distinguishing ice-rich and ice-poor permafrost to map ground temperatures and ground ice occurrence in the Swiss Alps, The Cryosphere, 13, 1925–1941, https://doi.org/10.5194/tc-13-1925-2019, 2019.

Krainer, K. and Mostler, W.: Hydrology of Active Rock Glaciers: Examples from the Austrian Alps, Arct. Antarct. Alp. Res., 34, 142–149, https://doi.org/10.1080/15230430.2002.12003478, 2002.

Krainer, K. and Mostler, W.: Flow velocities of active rock glaciers in the Austrian Alps, Geogr. Ann. A, 88, 267–280, https://doi.org/10.1111/j.0435-3676.2006.00300.x, 2006.

Krainer, K., Mostler, W., and Spötl, C.: Discharge from active rock glaciers, Austrian Alps: A stable isotope approach, Austrian J. Earth Sci., 100, 102–112, 2007.

Krainer, K., Bressan, D., Dietre, B., Haas, J. N., Hajdas, I., Lang, K., Mair, V., Nickus, U., Reidl, D., Thies, H., and Tonidandel, D.: A 10 300 year-old permafrost core from the active rock glacier Lazaun, southern Ötztal Alps (South Tyrol, northern Italy), Quaternary Res., 83, 324–335, https://doi.org/10.1016/j.yqres.2014.12.005, 2015.

Leibundgut, C., Maloszewski, P., and Külls, C.: Tracers in Hydrology, John Wiley & Sons, Ltd, 415 pp., https://doi.org/10.1002/9780470747148, 2009.

Li, M., Yang, Y., Peng, Z., and Liu, G.: Assessment of rock glaciers and their water storage in Guokalariju, Tibetan Plateau, The Cryosphere, 18, 1–16, https://doi.org/10.5194/tc-18-1-2024, 2024.

MeteoSwiss: Federal Office for Meteorology and Climatology, MeteoSwiss, https://www.meteoschweiz.admin.ch/service-und-publikationen/applikationen/messwerte-und-messnetze.html#lang=de&swisstopoApiKey=cpZJOL3HuO5yENksi97q¶m=messwerte-niederschlag-10min&station=SMM&chart=month, last access: 11 January 2024.

Moradi, H., Furrer, G., Michael, M., David, M., and Wanner, C.: Massive mobilization of toxic elements from an intact rock glacier in the Central Eastern Alps: insights on ice melt dynamics, Zenodo [data set], https://doi.org/10.5281/zenodo.10558549, 2024.

Muniz, I. P.: Freshwater acidification: its effects on species and communities of freshwater microbes, plants and animals, Proc. R. Soc. Ser. B-Bio., 97, 227–254, 1990.

Munroe, J. S. and Handwerger, A. L.: Contribution of rock glacier discharge to late summer and fall streamflow in the Uinta Mountains, Utah, USA, Hydrol. Earth Syst. Sci., 27, 543–557, https://doi.org/10.5194/hess-27-543-2023, 2023.

Nickus, U., Thies, H., Krainer, K., Lang, K., Mair, V., and Tonidandel, D.: A multi-millennial record of rock glacier ice chemistry (Lazaun, Italy), Front. Earth Sci., 11, 1141379, https://doi.org/10.3389/feart.2023.1141379, 2023.

Noetzli, J. and Pellet, C. (Eds.): Swiss Permafrost Bulletin 2022, PERMOS, 23 pp., https://www.permos.ch/publications (last access: 11 January 2024), 2023.

O'Donnell, J. A., Carey, M. P., Koch, J. C., Baughman, C., Hill, K., Zimmerman, C. E., Sullivan, P. F., Dial, R., Lyons, T., Cooper, D. J., and Poulin, B. A.: Metal mobilization from thawing permafrost to aquatic ecosystems is driving rusting of Arctic streams, Commun. Earth Environ., 5, 268, https://doi.org/10.1038/s43247-024-01446-z, 2024.

Parbhakar-Fox, A. and Lottermoser, B.: Principles of Sulfide Oxidation and Acid Rock Drainage BT – Environmental Indicators in Metal Mining, edited by: Lottermoser, B., Springer International Publishing, Cham, 15–34, https://doi.org/10.1007/978-3-319-42731-7_2, 2017.

Perruchoud, E. and Delaloye, R.: Short-Term Changes in Surface Velocities on the Becs-de-Bosson Rock Glacier (Western Swiss Alps), Grazer Schriften der Geogr. und Raumforsch., 43, 131–136, 2007.

Rist, A. and Phillips, M.: First results of investigations on hydrothermal processes within the active layer above alpine permafrost in steep terrain, Norsk Geogr. Tidsskr., 59, 177–183, https://doi.org/10.1080/00291950510020574, 2005.

Sannino, C., Qi, W., Rüthi, J., Stierli, B., and Frey, B.: Distinct taxonomic and functional profiles of high Arctic and alpine permafrost-affected soil microbiomes, Environ. Microbiome, 18, 1–22, https://doi.org/10.1186/s40793-023-00509-6, 2023.

Schmid, S. M., Fügenschuh, B., Kissling, E., and Schuster, R.: Tectonic map and overall architecture of the Alpine orogen, Eclogae Geol. Helv., 97, 93–117, https://doi.org/10.1007/s00015-004-1113-x, 2004.

Schmid, S. V.: Geologie des Umbrailgebiets, E–Periodica, 66, 101–210, https://doi.org/10.5169/seals-164185, 1973.

Shaw, C. A. and Tomljenovic, L.: Aluminum in the central nervous system (CNS): toxicity in humans and animals, vaccine adjuvants, and autoimmunity, Immunol. Res., 56, 304–316, https://doi.org/10.1007/s12026-013-8403-1, 2013.

SLF: Beschreibung automatische Stationen, Institute for Snow and Avalanche Research, https://www.slf.ch/de/lawinenbulletin-und-schneesituation/messwerte/beschreibung-automatische-stationen/, last access: 11 January 2024.

Steingruber, S. M., Bernasconi, S. M., and Valenti, G.: Climate Change-Induced Changes in the Chemistry of a High-Altitude Mountain Lake in the Central Alps, Aquat. Geochem., 27, 105–126, https://doi.org/10.1007/s10498-020-09388-6, 2021.

Swisstopo: Explanatory booklet of the Geological Atlas of Switzerland 1:25,000, Federal Office of Topography, https://shop.swisstopo.admin.ch/en/maps/geological-maps/explanatory-booklet-geological-atlas-switzerland-25000, last access: 11 January 2024a.

Swisstopo: GeoCover, Federal Office of Topography, https://www.swisstopo.admin.ch/en/geodata/geology/maps/geocover.html, last access: 11 January 2024b.

Tenthorey, G.: Perennial névés and the hydrology of rock glaciers, Permafrost Periglac., 3, 247–252, https://doi.org/10.1002/ppp.3430030313, 1992.

Thies, H., Nickus, U., Mair, V., Tessadri, R., Tait, D., Thaler, B., and Psenner, R.: Unexpected response of high alpine lake waters to climate warming, Environ. Sci. Technol., 41, 7424–7429, https://doi.org/10.1021/es0708060, 2007.

Thies, H., Nickus, U., Tolotti, M., Tessadri, R., and Krainer, K.: Evidence of rock glacier melt impacts on water chemistry and diatoms in high mountain streams, Cold Reg. Sci. Technol., 96, 77–85, https://doi.org/10.1016/j.coldregions.2013.06.006, 2013.

Thies, H., Nickus, U., Tessadri, R., Tropper, P., and Krainer, K.: Peculiar arsenic, copper, nickel, uranium, and yttrium-rich stone coatings in a high mountain stream in the Austrian alps, Austrian J. Earth Sci., 110, 7, https://doi.org/10.17738/ajes.2017.0012, 2017.

Todd, A. S., Manning, A. H., Verplanck, P. L., Crouch, C., McKnight, D. M., and Dunham, R.: Climate-change-driven deterioration of water quality in a mineralized watershed, Environ. Sci. Technol., 46, 9324–9332, https://doi.org/10.1021/es3020056, 2012.

Tolotti, M., Cerasino, L., Donati, C., Pindo, M., Rogora, M., Seppi, R., and Albanese, D.: Alpine headwaters emerging from glaciers and rock glaciers host different bacterial communities: Ecological implications for the future, Sci. Total Environ., 717, 137101, https://doi.org/10.1016/j.scitotenv.2020.137101, 2020.

Tolotti, M., Brighenti, S., Bruno, M. C., Cerasino, L., Pindo, M., Tirler, W., and Albanese, D.: Ecological "Windows of opportunity" influence biofilm prokaryotic diversity differently in glacial and non-glacial Alpine streams, Sci. Total Environ., 944, 173826, https://doi.org/10.1016/j.scitotenv.2024.173826, 2024.

Wagner, T., Kainz, S., Wedenig, M., Pleschberger, R., Krainer, K., Kellerer-Pirklbauer, A., Ribis, M., Hergarten, S., and Winkler, G.: Wasserwirtschaftliche Aspekte von Blockgletschern in Kristallingebieten der Ostalpen, RGHeavyMetal, BBK No. 101093, The University of Graz, 2019.

Wagner, T., Brodacz, A., Krainer, K., and Winkler, G.: Active rock glaciers as shallow groundwater reservoirs, Austrian Alps, Grundwasser, 25, 215–230, https://doi.org/10.1007/s00767-020-00455-x, 2020.

Wagner, T., Kainz, S., Krainer, K., and Winkler, G.: Storage-discharge characteristics of an active rock glacier catchment in the Innere Ölgrube, Austrian Alps, Hydrol. Process., 35, 1–16, https://doi.org/10.1002/hyp.14210, 2021a.

Wagner, T., Seelig, S., Helfricht, K., Fischer, A., Avian, M., Krainer, K., and Winkler, G.: Assessment of liquid and solid water storage in rock glaciers versus glacier ice in the Austrian Alps, Sci. Total Environ., 800, 149593, https://doi.org/10.1016/j.scitotenv.2021.149593, 2021b.

Wanner, C., Pöthig, R., Carrero, S., Fernandez-Martinez, A., Jäger, C., and Furrer, G.: Natural occurrence of nanocrystalline Al-hydroxysulfates: Insights on formation, Al solubility control and As retention, Geochim. Cosmochim. Ac., 238, 252–269, https://doi.org/10.1016/j.gca.2018.06.031, 2018.

Wanner, C., Moradi, H., Ingold, P., Cardenas Bocanegra, M. A., Mercurio, R., and Furrer, G.: Rock glaciers in the Central Eastern Alps – How permafrost degradation can cause acid rock drainage, mobilization of toxic elements and formation of basaluminite, Global Planet. Change, 227, 104180, https://doi.org/10.1016/j.gloplacha.2023.104180, 2023.

Williams, M. W., Knauf, M., Caine, N., Liu, F., and Verplanck, P. L.: Geochemistry and source waters of rock glacier outflow, Colorado Front Range, Permafrost Periglac., 17, 13–33, https://doi.org/10.1002/ppp.535, 2006.

Williamson, M. A. and Rimstidt, J. D.: The kinetics and electrochemical rate-determining step of aqueous pyrite oxidation, Geochim. Cosmochim. Ac., 58, 5443–5454, https://doi.org/10.1016/0016-7037(94)90241-0, 1994.

Zarroca, M., Roqué, C., Linares, R., Salminci, J. G., and Gutiérrez, F.: Natural acid rock drainage in alpine catchments: A side effect of climate warming, Sci. Total Environ., 778, 146070, https://doi.org/10.1016/j.scitotenv.2021.146070, 2021.

Remarks from the language copy-editor

CE1   Please note the slight edits.

CE2   Please note the slight edits.

Remarks from the typesetter

TS1   Note that changes in the scientific content require editor approval. Please provide a short explanation regarding this correction that can be forwarded by us to the editor.